Published in "European Journal of Neuroscience 46(8): 2406–2415, 2017"
which should be cited to refer to this work.

Ipsilateral corticotectal projections from the primary, premotor and supplementary motor cortical areas in adult macaque monkeys: a quantitative anterograde tracing study

Michela Fregosi and Eric M. Rouiller
Platform of Translational Neurosciences, Fribourg Cognition Center, Department of Medicine, Swiss Primate Competence Center for Research (SPCCR), University of Fribourg, Chemin du Musée 5, Fribourg 1700, Switzerland

Keywords: anterograde tracing, midbrain, motor cortex, non-human primate, premotor cortex

Abstract

The corticotectal projection from cortical motor areas is one of several descending pathways involved in the indirect control of spinal motoneurons. In non-human primates, previous studies reported that cortical projections to the superior colliculus (SC) originated from the premotor cortex (PM) and the primary motor cortex, whereas no projection originated from the supplementary motor area (SMA). The aim of the present study was to investigate and compare the properties of corticotectal projections originating from these three cortical motor areas in intact adult macaques (n = 9). The anterograde tracer biotinylated dextran amine was injected into one of these cortical areas in each animal. Individual axonal boutons, both *en passant* and *terminaux*, were charted and counted in the different layers of the ipsilateral SC. The data confirmed the presence of strong corticotectal projections from the PM. A new observation was that strong corticotectal projections were also found to originate from the SMA (its proper division). The corticotectal projection from the primary motor cortex was quantitatively less strong than that from either the premotor or SMAs. The corticotectal projection from each motor area was directed mainly to the deep layer of the SC, although its intermediate layer was also a consistent target of fairly dense terminations. The strong corticotectal projections from non-primary motor areas are in position to influence the preparation and planning of voluntary movements.

Introduction

The corticospinal (CS) projection, originating from multiple motor cortical areas, plays a major role in manual dexterity, a specialty of primates (see, e.g., Lawrence & Hopkins, 1976; Lawrence *et al.*, 1985; Lemon & Griffiths, 2005; Courtine *et al.*, 2007; Lemon, 2008). The motor cortical areas also influence other descending pathways via their corticobulbar (or corticoreticular), corticorubral and corticotectal projections (Kuypers, 1981; Lemon, 2008, 2016). In a recent study (Fregosi *et al.*, 2017), the corticobulbar projection was characterized in intact adult macaque monkeys by visualizing the axonal boutons in the Ponto-Medullary Reticular Formation (PMRF) labelled with injections of the anterograde tracer biotinylated dextran amine (BDA) in either the primary motor cortex (M1), the premotor cortex (PM) or the supplementary motor area (SMA). The non-primary motor areas (PM and SMA) exhibited a stronger corticobulbar projection than that originating from M1 (Fregosi *et al.*, 2017).

The goal of the present investigation was to assess the respective contribution of these three motor cortical areas to the corticotectal projection in adult macaques. An early degeneration study of Kuypers & Lawrence (1967) reported projections to the superior colliculus (SC) from premotor and motor cortical areas. Based on retrograde tracer (HRP) injections in the SC of macaque monkeys, a significant motor corticotectal projection originating from layer V of PM was observed, terminating in the intermediate and deep layers of SC (Fries, 1984, 1985). The corticotectal projection from PM was confirmed by injections of the anterograde tracer BDA in the dorsal PM (Distler & Hoffmann, 2015) or in the ventral PM (F5 area; Borra *et al.*, 2010, 2014). Both studies reported that the projections from PM indeed terminate in the intermediate and deep layers of the SC. In addition to PM, corticotectal neurons were observed in M1 as a result of retrograde tracer injections in SC (Fries, 1984, 1985). The corticotectal projection from M1 was confirmed with anterograde tracers injected in the orofacial region of

Correspondence: Professor Eric M. Rouiller, as above.
E-mail: Eric.Rouiller@unifr.ch

The associated peer review process communications can be found in the online version of this article.

M1 (Tokuno *et al.*, 1995). Corticotectal neurons in M1 layer V were generally of small size whereas they were, on average, larger and more numerous in PM (Fries, 1984, 1985). Interestingly, as a result of retrograde tracer injections in SC, there were no labelled neurons in SMA (Fries, 1984, 1985). The goal of the present analysis was to extend previous corticotectal anterograde tracing data of PM (Borra *et al.*, 2010, 2014; Distler & Hoffmann, 2015) to M1 and SMA, with the hypothesis of a projection strength gradient decreasing from PM to M1 and from M1 to SMA.

The primate SC is involved in multisensory and sensorimotor integration (Stein *et al.*, 2009; Wurtz, 2009 for review), and is comprised of seven concentric layers: the zonal, superficial grey layer (SCsup), optical zone (InSup), intermediate grey layer (SCint), intermediate white layer (InWh), deep grey layer (SCdeep) and deep white layer (DpWh; e.g. Gandhi & Katnani, 2011). The superficial grey layer receives inputs from the retina and visual areas (Lock *et al.*, 2003) whereas its intermediate and deep grey layers receive more widespread corticotectal projections, involving sensory (vision, hearing, somatosensory) and motor functions (e.g. Fries, 1984, 1985; Tokuno *et al.*, 1995; Lock *et al.*, 2003; Collins *et al.*, 2005; Borra *et al.*, 2014; Distler & Hoffmann, 2015). In the deep layers of the SC, visual and auditory information is integrated to create a sensory map of the surrounding space (Squire *et al.*, 2013). Furthermore, there are neurons in SC deep layers which were reported to be reach-related (Werner, 1993; Werner *et al.*, 1997a,b) or hand-object related (Nagy *et al.*, 2006); electrical microstimulation of the deep SC generates arm movements (Philipp & Hoffmann, 2014). The deep layers of SC are also the zone of origin of the tectospinal tract (Castiglioni *et al.*, 1978; Nudo & Masterton, 1988, 1989; Nudo *et al.*, 1993; see also Abrahams & Rose, 1975 for the cat). Besides comparing the strength of corticotectal projections originating from distinct motor cortical areas (PM, M1, SMA), the present anterograde tracing experiments are also suitable to determine whether the laminar distribution of axonal boutons in the SC varies between M1 and PM, and possibly also SMA in case the latter is the origin of a corticotectal projection.

Methods

All experimental procedures were in compliance with European and applicable Swiss regulations. The experiments were conducted in respect of ethical guidelines (ISBN 0-309-05377-3, 1996) and the Swiss legislation on animal care and protection, as evidenced by the corresponding animal experimentation authorizations delivered by the local (Canton of Fribourg) and federal veterinary authorities (No 156-08E, 156-02, 156-00, 44-92-3). The materials and methods are similar to those described in detail in a recent report on the corticobulbar projections from PM, M1 and SMA in intact adult macaque monkeys (Fregosi *et al.*, 2017). In addition to the same seven monkeys (*Macaca fascicularis*) subjected to BDA (MW = 10 000) injections in PM (n = 3), in M1 (n = 3) and in the caudal SMA (SMA-proper; n = 1), the present material was extended to two more animals (*Macaca mulatta*) one injected in SMA-proper and the other in the rostral SMA (pre-SMA). The individual properties of these nine macaques are listed in Table 1. The BDA injection sites were illustrated for the seven cases used in the recent study of the corticobulbar projection (Fregosi *et al.*, 2017). The injection site of the additional monkey with BDA deposited in SMA-proper has been illustrated previously as well (Tanné-Gariépy *et al.*, 2002a; their fig. 1 – Mk3; also reported here in Fig. 4B). Finally, the second additional monkey was injected with BDA in pre-SMA (Fig. 1), without spread to SMA-proper as there was no connection with M1, in line with previous data for F6 (corresponding to pre-SMA – Luppino *et al.*, 1993).

TABLE 1. Individual data for the nine monkeys included in the present study

	PM-1	PM-2	PM-3	M1-1	M1-2	M1-3	SMA-1	SMA-2	Pre-SMA
	Mk-R13	Mk-R12	Mk-CH	Mk-Z182	Mk-M310	Mk-M93-80	Mk-M93-81	Mk-BS	Mk-IU
BDA injection in	PMd/PMv	PMd	PMd/PMv	M1	M1	M1	SMA	SMA	Pre-SMA
Age at sacrifice	4.5	6	10	7.5	8.5	4	4	6	9
Weight	4	4	6	10	10	4	4	7	9
Sex	Female	Female	Male	Male	Male	Male	Male	Male	Male
Species	Fasc.	Fasc.	Fasc.	Fasc.	Fasc.	Fasc.	Fasc.	Mul.	Mul.
No. of series of sections	5	5	5	8	8	7	7	7	8
Intersection interval (μm)	250	250	250	400	400	350	350	350	400
BDA volume injected (μL)	8.8	7.2	8	25.5	22.5	10	10	4	8
No. of BDA sites injected	11	9	10	17	15	7	6	4	8
Body territory injected*	Large	Large	Large	Forelimb	Forelimb	Hand	Hand	Hand	–
Raw no. boutons in SC	10 401	4469	3034	361	257	470	1625	4224	0
Corrected no. boutons in SC†	10 401	4469	3034	578	411	658	2275	5914	0
Corrected no. boutons in SCint	6358	1762	912	206	32	22	325	1116	0
Corrected no. boutons in SCdeep	3284	1938	1684	272	336	547	1044	2965	0
No. labelled corticospinal axons	1802	1473	1201	950	703	3195	2160	908	0
Normalized no. boutons in SC‡	5772	3034	2526	608	585	206	1053	6513	0

BDA, biotinylated dextran amine; ICMS, intracortical microstimulation; PM, Premotor cortex; PMv, ventral premotor cortex; SC, Superior Colliculus; SCint, intermediate nucleus of SC; SCdeep, deep nucleus of SC; Fasc., *Macaca fascicularis*; Mul., *Macaca mulatta*. In the top row, the IDs of monkeys are as in Fregosi *et al.* (2017) for seven of them (seven left most columns), with two newly inserted monkeys (two rightmost columns). The second row gives original IDs used in the laboratory, as well as in earlier reports. *In PM, the BDA injections covered most of the targeted areas (see Fregosi *et al.*, 2017), namely PMd in Mk-R12 and PMd/PMv in the other two monkeys (Mk-R13 and Mk-CH). In M1, in two monkeys (Mk-Z182 and Mk-M310), BDA was injected in absence of ICMS (based on sulci) in territories including most likely the hand and the arm territories; In Mk-M93-80, BDA was injected in the hand area delineated with ICMS. The hand area, also identified by ICMS, was injected with BDA in SMA-proper (Mk-M93-81 and Mk-BS). In pre-SMA (Mk-IU), BDA was deposited in the area as defined in Liu *et al.* (2002) as the rostral part of SMA. †The raw number of axonal boutons in SC was corrected to take into account the differences in intersection interval, as explained in the Methods (no corrections for the three monkeys with injections in PM taken as reference – 250 μm intersection interval). ‡In each monkey, the number of axonal boutons in SC was normalized according to the number of corticospinal labelled axons, as explained in the Methods.

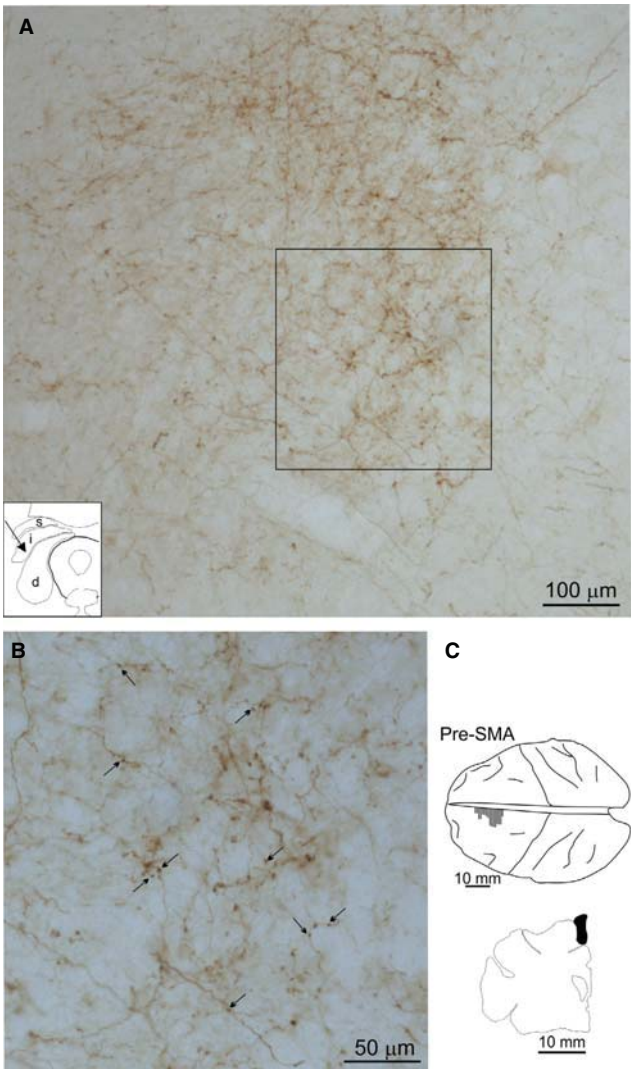

FIG. 1. (A, B) Photomicrographs showing typical biotinylated dextran amine (BDA) anterogradely labelled axonal terminal fields in the ipsilateral superior colliculus (SC) after injection of BDA in PM (taken from monkey PM-1), and at two magnifications. The terminal field illustrated is located in the intermediate layer of the SC, as indicated in the inset on the bottom left of panel A (arrow; s = superior layer of SC; i = intermediate layer of SC; d = deep layer of SC). The rectangle in panel A shows the zone illustrated at higher magnification in panel B, where a few axonal boutons are pointed by arrows as example. (C) Reconstruction of the BDA injection site in monkey Pre-SMA, located in pre-SMA, as shown on a top view of the brain – hatched zone on the left hemisphere adjacent to the midline (other injection sites reported in earlier studies, as mentioned in the Methods section). In the bottom, drawing of a frontal section taken in the middle of the injection site, which appears as a black spot.

All measures were taken to minimize pain and constraints on the animals, and their number was also kept as low as possible, in particular using the same cases (namely BDA injections in various motor cortical areas) to study distinct connection/projection systems (Rouiller *et al.*, 1994, 1996, 1998, 1999; Liu *et al.*, 2002; Tanné-Gariépy *et al.*, 2002a,b; Freund *et al.*, 2007; Schmidlin *et al.*, 2009; Fregosi *et al.*, 2017; Innocenti *et al.*, 2017).

The anaesthesia, analgesia, surgical, injection, euthanasia and histological procedures were the same as reported in detail recently (Fregosi *et al.*, 2017). Sections of the brain (including the midbrain) were cut at 50 µm in the frontal plane using a freezing microtome and collected in 5–8 series (see Table 1). One series of sections was processed to visualize BDA (Rouiller *et al.*, 1994), and sections of this series including the SC were analysed using Neurolucida software (version 11; MicroBrightField Inc.) on an Olympus light microscope interfaced with a computer (see Fregosi *et al.*, 2017 for detail). The analysed intersection intervals ranged from 250 to 400 µm (Table 1). The BDA section outline was reconstructed at a magnification of 40×. Then the section was scanned at 100× for stem BDA-labelled axons and finally re-scanned at 200× to chart axonal boutons *en passant* and *terminaux*. Boutons were defined as an enlargement of an axonal branch in a terminal field exhibiting a diameter of at least twice that of the axon segment preceding the bouton itself (Fig. 1; same criterion as in Fregosi *et al.*, 2017 for the corticobulbar projection). The SC ipsilateral to the BDA-injected hemisphere was scanned, in addition to parts of neighbouring territories in the peri-acqueductal grey (PAG) medially and the mesencephalic reticular formation ventrally (as the precise border of the SC medially and ventrally did not appear on BDA-stained sections). Axonal boutons were rare in the contralateral SC, which was scanned manually to count them. Each BDA-analysed section was then superimposed to an adjacent Nissl-stained section, used to delineate the nuclei of the midbrain, including the distinct regions of the SC, especially the superficial (SCsup), the intermediate (SCint) and the deep (SCdeep) layers. The intermingled zones Op, InWh and DpWh were identified at the same time, based on the macaque brain atlas (Paxinos *et al.*, 2000). The final superimposition of Nissl and BDA sections was performed using CorelDraw X7 software. The numbers of BDA-labelled boutons were established in each of the six sublayers of the SC. As the section area to scan is restricted (mostly the ipsilateral SC), and the axonal terminal fields labelled with BDA are usually of small extent, it was possible to visualize and chart every individual axonal bouton, *en passant* or *terminal*. This quantification method based on exhaustive plotting was used instead of stereology to allow comparison with a previous study on corticoreticular projections using the same cases and the same quantification method (Fregosi *et al.*, 2017).

As the brains were cut at 50 µm and collected in a variable number of series of histological sections across monkeys (ranging from 5 to 8; see Table 1), the numbers of axonal boutons were corrected (Fig. 5A), taking as reference brains cut in five series of sections (PM-1, PM-2 and PM-3). The other monkeys with a higher number of series (7 or 8) were under-quantified and therefore, the numbers of axonal boutons were multiplied by 1.4 or 1.6, respectively.

Due to variability in BDA injection volume, precise position, tracer uptake and transport, the data were further normalized according to the number of CS axons counted in most cases on one section just above the pyramidal decussation (Table 1). However, in a previous study (Rouiller *et al.*, 1996; including the monkeys M1-3 and SMA-1), we had performed repeated counts of CS axons in adjacent sections, yielding comparable numbers. As both the CS and corticotectal projections arise from layer V in the frontal lobe (Fries, 1984, 1985), a normalization based on the CS axons' number represents a fairly reliable indicator of how much of the BDA injection indeed involved cortical layer V in PM, M1 and SMA. Therefore, the normalization consisted of dividing the number of BDA-labelled axonal boutons by the corresponding number of BDA-labelled CS axons in the same animal, multiplied by 1000 (Table 1; Fig. 5B). One thousand corresponds to an approximate order of magnitude of the number of CS axons obtained across our monkey population (range 703 to 3195, see Table 1).

Results

In three monkeys, we found a significant corticotectal projection from PM to the SC (PM-1, PM-2 and PM-3). As illustrated for

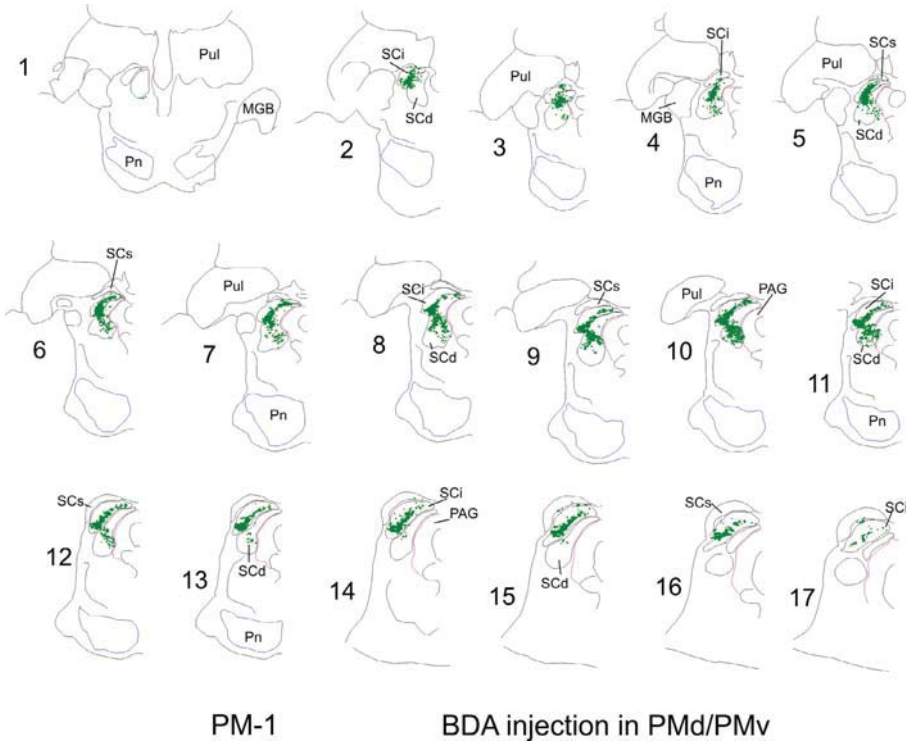

FIG. 2. Serial sections of half of the midbrain (ipsilateral to the BDA injection in PM; monkey PM-1) arranged from rostral to caudal (1–17). The most rostral section (#1) shows both sides. The intersection interval is 250 μm. The green dots represent the location of the charted BDA-labelled axonal boutons in the superior colliculus (SC). SCs, superior layer of SC; SCi, intermediate layer of SC; SCd, deep layer of SC. See Fig. 3 for location of the three intermingled zones of SC (Op, InWh and DpWh). See also list of abbreviations.

PM-1 (Fig. 2), following the injection of BDA in both PMd and ventral premotor cortex (PMv), most axonal boutons were observed caudally in the intermediate layer of SC (SCint; sections 1–5). Going more rostrally (sections 6–16), the SCint remained a dense target, and axonal boutons were numerous in the deep layer of SC (SCdeep) as well. Table 1 indicates the number of axonal boutons charted in SCint and SCdeep, with a predominance of SCint. PM-3 also received BDA injections in PMd and PMv, and showed a topographically comparable distribution of axonal boutons along the rostrocaudal axis (data not shown), although there were more boutons in SCdeep than in SCInt (Table 1). The third BDA injection in PM (restricted to PMd; monkey PM-2) yielded a pattern of bouton distribution (not shown) comparable to PM-3, with more boutons in SCdeep than SCint (Table 1). Overall, the corticotectal projection from PM covers the entire rostrocaudal extent of SC (Fig. 2).

Following BDA injections in M1 (cases M1-1, M1-2 and M1-3), the corticotectal projection appeared less strong than that for PM and covered a more restricted rostrocaudal extent of SC, with few or no axonal boutons in the most caudal part of SC (Fig. 3 illustrating case M1-1). Although some boutons were present in SCint, most of them were found in SCdeep. The difference between SCdeep (numerous boutons) and Scint (few boutons) was even more prominent in M1-2 and M1-3 (not shown, but see Table 1). Note that in one (M1-3) of the three monkeys injected in M1, BDA was deposited specifically in the hand representation, as identified with intracortical microstimulation (ICMS; Table 1).

An unexpected finding, based on the literature, was the presence of a significant corticotectal projection originating from SMA-proper as illustrated for SMA-2 in Fig. 4. As for PM, the distribution of axonal boutons covered most of the rostrocaudal extent of SC. They were found mostly in SCint and SCdeep, with a predominance of the latter (Table 1) in a proportion of 1 : 3 approximately in both SMA cases. A topographically similar distribution of BDA-labelled axonal boutons in SC was found in a second monkey (SMA-1) also injected in SMA-proper (not shown; see however Fig. 6). Note that in these two monkeys (SMA-2 and SMA-1), the BDA injection was targeted to the hand area identified with ICMS (Table 1). In sharp contrast, BDA injection in pre-SMA (monkey Pre-SMA) did not give rise to corticotectal or corticospinal projections (Table 1).

The numbers of axonal boutons counted in the SC for each motor area are compared in Table 1 and Fig. 5. The raw numbers of axonal boutons were corrected according to the interval of section sampling across monkeys (see Methods). The corrected numbers of axonal boutons in SC were highest for the PM, somewhat lower for the SMA-proper and much lower for M1 (Fig. 5A).

To further compare the strength of the corticotectal projections originating from PM, M1 or SMA-proper, the total corrected numbers of axonal boutons in SC were normalized based on the number of CS axons obtained for the same BDA injection (see Methods). After normalization, the conclusions based on the corrected numbers of axonal boutons (Fig. 5A) were largely validated (Fig. 5B). The corticotectal projection from M1 is considerably weaker than those originating from the two premotor areas (PM and SMA-proper). Furthermore, the normalized data along with the inter-individual variability among animals suggest that the strength of the corticotectal projections from the PM and SMA (Fig. 5B) is comparable.

SCdeep was the main laminar target in all monkeys, except PM-1 (Fig. 6, Table 1). In most cases, there was also a substantial projection terminating in SCint. This projection, however, was quite variable from one animal to the next, especially for the projections originating from M1 and to a lesser extent for those from PM. Axonal boutons were also found in the three intermingled zones of SC

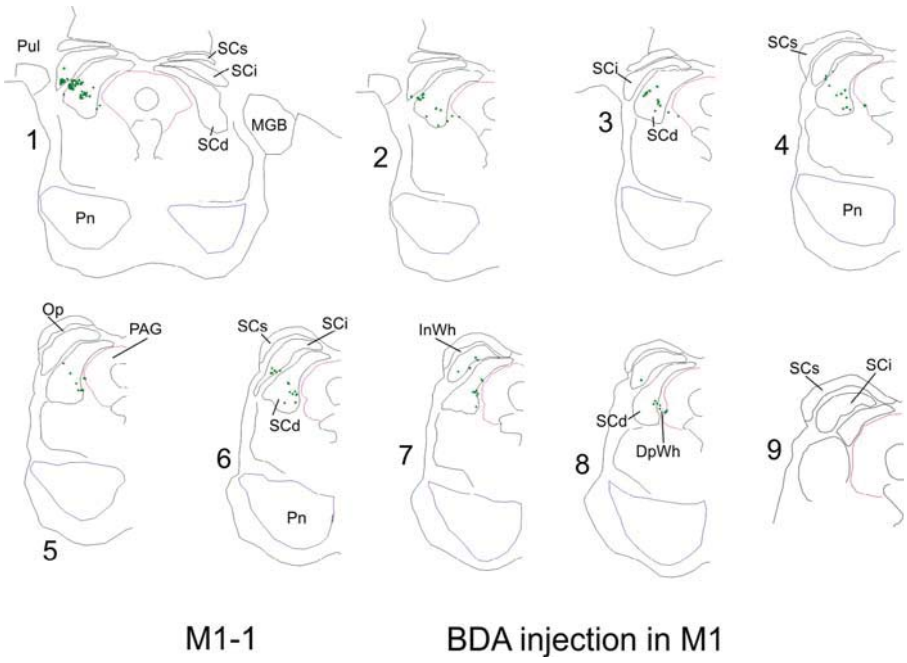

FIG. 3. Serial sections of half of the midbrain (ipsilateral to the BDA injection in M1; monkey M1-1) arranged from rostral to caudal (1–9). The most rostral section (#1) shows both sides. The intersection interval is 400 µm. The green dots represent the location of the charted BDA-labelled axonal boutons in the superior colliculus (SC). SCs, superior layer of SC; SCi, intermediate layer of SC; SCd, deep layer of SC. This Figure shows the location of the three intermingled zones of SC (Op, InWh, DpWh). See also list of abbreviations.

Op, InWh and DpWh, most often in the latter two (Fig. 6). In contrast, the superior layer of SC (SCsup) exhibited axonal boutons very rarely following BDA injection in PM or SMA and none following injection in M1. Irrespective of the cortical area of origin, the BDA-labelled axonal boutons were found mostly laterally in SCint (although with some extension medially in some sections) and in the ventrolateral sector of SCdeep (Figs 2–4). Note also that BDA-labelled axonal boutons were observed in the neighbouring PAG matter (medial to SC) and in the mesencephalic reticular formation (ventral to SC), but they were not systematically charted and counted.

The corticotectal projections from PM, SMA-proper or M1 appeared to be mostly restricted to the ipsilateral SC. However a few BDA-labelled axons were found in the SC contralateral to the injected hemisphere, most of these axons were passing stem axons that did not emit boutons, *en passant* or *terminaux*. However, rare axonal boutons were observed in SCint and SCdeep contralaterally. When present, these corticotectal axonal boutons in the contralateral SC were located in regions that mirrored the main projection territories in the ipsilateral SC. The percentage of the total number of axonal boutons observed in the contralateral SC ranged from 0.0% to 1.6% in all but one monkey (SMA-1) where the contralateral percentage was 4.8%.

Discussion

The present analyses demonstrate that the PM, SMA-proper and M1 have significant projections to the ipsilateral SC. The major new finding is that the SMA-proper gives rise to a substantial corticotectal projection (Fig. 4; Table 1). This SMA projection is similar in strength to that of the PM and considerably stronger than that originating from M1 (Fig. 5). The presence of corticotectal projections from the SMA was unexpected as a prior retrograde tracing study failed to observe labelling in the SMA after HRP injections into the SC (Fries, 1984, 1985). Our observations are consistent with and extend prior studies (Borra *et al.*, 2010, 2014; Distler & Hoffmann, 2015) that examined corticotectal projections from PM. Our quantitative analysis, like those prior qualitative studies, found that SCint and SCdeep are the major targets of the corticotectal projection originating from PM whereas there was only a very weak corticotectal projection originating from motor cortical areas to SCsup. Overall, our observations demonstrate that corticotectal projections originate from more widespread regions of the cortical motor areas in the frontal lobe than previously recognized and that these projections target the deep layers of the SC.

The failure of prior studies (Fries, 1984, 1985) to detect projections from the SMA to the SC may result from two factors. First, Fries used HRP as retrograde tracer, which is a less sensitive tracing method than BDA. Second, most of his HRP injections in SC did not include the deepest layers of the SC where we found the heaviest projections from the SMA (Figs 4 and 6). Thus, his injections sites may have largely avoided the sites with the densest SMA terminations.

The present study, like recent reports (Borra *et al.*, 2010, 2014; Distler & Hoffmann, 2015), took advantage of the BDA tracing technique which allows visualization of axonal boutons within axon terminal fields. Furthermore, we could quantify the numbers of corticotectal boutons due to the spatially limited and relatively sparse terminal fields. Possible limitations of this quantitative analysis reside in variations of BDA injection sites, uptake and transport as well as the different sampling intervals of histological sections across monkeys. We attempted to attenuate these possible limitations by correcting for section sampling intervals and by normalizing the data based on CS axon counts (Fig. 5; see Fregosi *et al.*, 2017 for a more complete discussion of the normalization procedure). One limitation of our normalization procedure is that the corticotectal projections originate from limited territories of PM or M1 (Fries, 1984, 1985) whereas the BDA injection may spread beyond the cortical

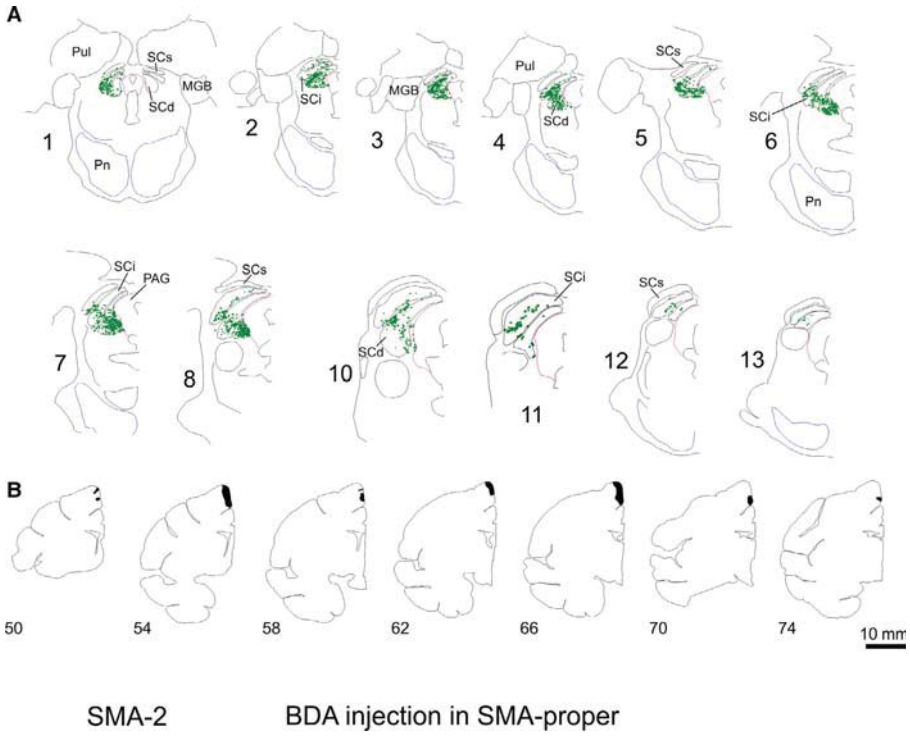

FIG. 4. (A) Serial sections of half of the midbrain (ipsilateral to the BDA injection in SMA; monkey SMA-2) arranged from rostral to caudal (1–13). The most rostral section (#1) shows both sides. The intersection interval is 400 μm. The green dots represent the location of the charted BDA-labelled axonal boutons in the superior colliculus (SC). SCs, superior layer of SC; SCi, intermediate layer of SC; SCd, deep layer of SC. See Fig. 3 for location of the three intermingled zones of SC (Op, InWh and DpWh). See also list of abbreviations. (B) Sections illustrating the location and extent of the BDA injection site (black area) for the case SMA-2. Sections are arranged from rostral (left: section 50) to caudal (right: section 74).

territories projecting to the SC. This would result in an elevated CS axons' count that comprised CS axons originating both within and outside of the SC projection territory. Consequently, the normalized number of boutons in SC would be decreased. In addition, the PM and SMA tend to emit a slightly lower number of CS axons than M1 (Dum & Strick, 1991), which would increase the normalized number of boutons from PM and SMA as compared to M1.

In the interpretation of the normalized data, there are three possible scenarios: (i) the raw data do not show any difference between the cortical areas of origin, but the normalized data do. In such a case, concerns about conclusions based on normalized data only are fully legitimate; (ii) the raw data show a difference between the cortical areas of origin, but not the normalized data. In such a case, variability among injections sites may be a concern; (iii) both the raw data and the normalized data go clearly in the same direction, as it is the case in the present study. The normalized data then represent an additional and consistent approach to the raw data. The trend in the normalized number of boutons among the motor areas is the same as the trend in the corrected raw data (Fig. 5). Therefore, normalized data support the conclusion derived from the raw data, namely that the PM and SMA have stronger projections to the SC than does M1.

Although the BDA labelling in the contralateral SC was restricted to a few passing stem axons, rare axonal boutons were also observed, representing around 1% of the total corticotectal projection. This is in line with a previous study reporting a contralateral corticotectal projection from PM, based on retrograde tracing data (Distel & Fries, 1982). Borra *et al.* (2014) also reported a contralateral projection to SC from the area F5. The present study extends these data to a contralateral projection to SC originating from SMA and, to a lesser extent, from M1. As far as bilaterality is concerned, the motor corticotectal projection appears to be highly lateralized (vast predominance of ipsilateral projection to SC – around 99%), in contrast to the corticobulbar (corticoreticular) projection (Fregosi *et al.*, 2017). The latter is clearly more bilateral, although there was some ipsilateral bias when originating from PM or SMA (50–67%), whereas the contralateral projection predominated when originating from M1 (58–71%). With respect to laterality, the corticospinal projection, containing about only 10% of uncrossed (ipsilateral) axons, sharply contrasts with the motor corticotectal projection mostly limited to the ipsilateral side.

The corticotectal projection from M1 remains somewhat controversial, at least with respect to its strength, which is certainly lower than that coming from PM. The corticotectal projection from M1 may vary depending on the body territory of origin. It was reported to be clearly stronger from the orofacial region of M1 than from the forelimb and hindlimb territories of M1 yielding 'very sparsely detected' labelled fibres in SC (Tokuno *et al.*, 1995). Such sparse labelling in SC was interpreted by Borra *et al.* (2014) as a lack of projection from the M1 hand area to the SC, in line with previous reports (e.g. Monakow *et al.*, 1979; Shook *et al.*, 1990). The present study confirms the existence of a corticotectal projection from M1, previously reported by Fries (1984, 1985), with evidence that it applies to the hand/arm territory as well, although less strong than from the face region (Tokuno *et al.*, 1995). Nevertheless, the corticotectal projection from M1 remains fairly modest in comparison with that arising from non-primary motor areas (PM and SMA). Note however that Tokuno *et al.* (1995) reported a corticotectal projection from the orofacial region of M1 terminating mostly in the intermediate layer of SC, whereas the present study shows a corticotectal projection mostly from the forelimb M1 area terminating predominantly in the deep layer of SC (Table 1). This layer difference

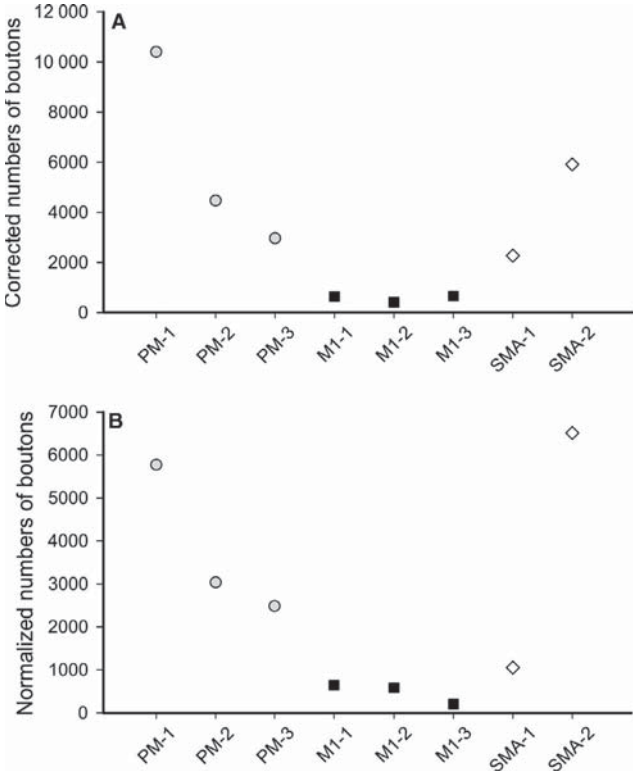

FIG. 5. (A) Comparison of the corrected numbers of BDA-labelled axonal boutons in SC (see Table 1) across monkeys and motor cortical area of origin. The identity of each monkey is given along the abscissa. (B) Same data but after normalization with respect to the number of BDA-labelled corticospinal axons (see Table 1 and as explained in the Methods section). SMA reads here for SMA-proper (the caudal SMA). Pre-SMA is not represented (monkey Pre-SMA) as there was no corticotectal projection in that monkey.

argues in favour of a somewhat distinct role played by the SC with respect to the control of movements, involving either the face or the arm/hand.

The corticotectal projection from SMA-proper is derived from two cases (SMA-1 and SMA-2), exhibiting different numbers of boutons in SC, about six times more in SMA-2, although the BDA injections were targeted in both monkeys to the hand representation. However, the rostrocaudal extent of the BDA injections sites in SMA-2 is larger than in SMA-1, possibly explaining this difference, especially if BDA spread from the hand area to the head representation in SMA-2, considering the functional significance of the SC in the control of the head movements.

The strength gradient of corticotectal projections observed here (Fig. 5), namely PM = SMA > M1, is reminiscent to that observed for the corticobulbar projection to PMRF (Fregosi *et al.*, 2017), at least for the weak projection originating from M1. In both cases, the terminal zones of the corticofugal (corticotectal and corticobulbar) projections match the location of the tectospinal neurons (Castiglioni *et al.*, 1978; Nudo & Masterton, 1989; Nudo *et al.*, 1993) and of the reticulospinal neurons in PMRF (Kneisley *et al.*, 1978; Nudo & Masterton, 1988; Sakai *et al.*, 2009; Borra *et al.*, 2010; Fregosi *et al.*, 2017), respectively. As a result, the corticotectal and corticobulbar projections originating from PM, SMA and M1 are in a position to indirectly influence spinal motoneurons via the mesencephalon and brainstem, in parallel to the direct corticospinal components originating from the same three motor cortical areas (e.g. Dum & Strick, 1991, 1996; He *et al.*, 1993, 1995; Rouiller *et al.*, 1996). However, the CS component from M1 outnumbers that coming from the PM or SMA (Dum & Strick, 1991, 1996; Rouiller *et al.*, 1996), whereas the projection strength is reversed (stronger projections from the PM and SMA than from M1) for the corticotectal (present study) and corticobulbar projections (Fregosi *et al.*, 2017). The gradient of corticotectal and corticoreticular (Fregosi *et al.*, 2017) projections in terms of strength with respect to their origin (PM ≥ SMA > M1) interestingly matches further gradients across premotor versus primary motor areas. In particular, the corticocortical connections of PM and SMA are more widespread than those of M1 (Morecraft *et al.*, 2012, 2015). Furthermore, the cytoarchitecture of PM – SMA – M1 exhibits gradual changes in laminar organization through premotor, supplementary motor and primary motor areas (Morecraft *et al.*, 2012, 2015; Barbas & Garcia-Cabezas, 2015). These anatomical and connectional gradients are likely to also reflect functional gradients (Markov *et al.*, 2014), corresponding to largely segregated functions in the control of voluntary movements across the premotor areas and the primary motor area.

Functionally, as the non-primary motor cortical areas are more specialized than M1 for preparation and programming of voluntary movements, both the corticotectal and corticobulbar projections from PM and SMA may send an early and fairly prominent information regarding the intended action, possibly useful to elaborate posture adaptation from the mesencephalic (SC) and brainstem (PMRF) motor centres, which belong to the ventromedial descending projection group (Lemon, 2008), biased towards proximal and trunk muscles. M1 appears to be more involved in the output via the CS projection, although small components are present in the corticotectal and corticobulbar projections, but most likely are related to movement execution.

Although they belong to the ventromedial descending projection system (Lemon, 2008), the corticotectal and corticobulbar projections are interfaced with the tectospinal and reticulospinal projections, which are involved not only in the control of posture, but also in reaching movements (e.g. Werner, 1993; Werner *et al.*, 1997a,b; Stuphorn *et al.*, 1999, 2000; Buford & Davidson, 2004; Davidson & Buford, 2004, 2006; Davidson *et al.*, 2007; Philipp & Hoffmann, 2014). Furthermore, these two systems of descending projections were found to be involved in the control of distal (hand) muscles such as during grasping (Nagy *et al.*, 2006; Riddle *et al.*, 2009; Riddle & Baker, 2010; Soteropoulos *et al.*, 2012). For the corticotectal projection and the related tectospinal projection, due to the known multisensory and sensorimotor integrative properties of the SC (see, e.g., Stein *et al.*, 2009; Wurtz, 2009 for review), their main functional contribution may well remain in the task of coordinating movements of arm/hand with those of eyes and head (including the neck), in order to generate complex and well-controlled behaviours to interact with objects of interest in a constantly changing environment. In the cat for instance, it has been shown that afferents from neck muscles and from extraocular muscles converge in the SC on cells of origin of the tectospinal tract (Abrahams & Rose, 1975).

From an evolutionary point of view (Nudo & Masterton, 1989), the tectospinal projection in the non-human primate represents quantitatively a minor descending projection in comparison with the more massive corticospinal and rubrospinal projections. The size of the tectospinal projection does not correlate with good vision, manual dexterity or hand–eye coordination (Nudo & Masterton, 1989). As a consequence, the moderate number of corticotectal axon terminals observed in the present study suggests that these projections may contribute to a motor-based regulation of intrinsic neuronal

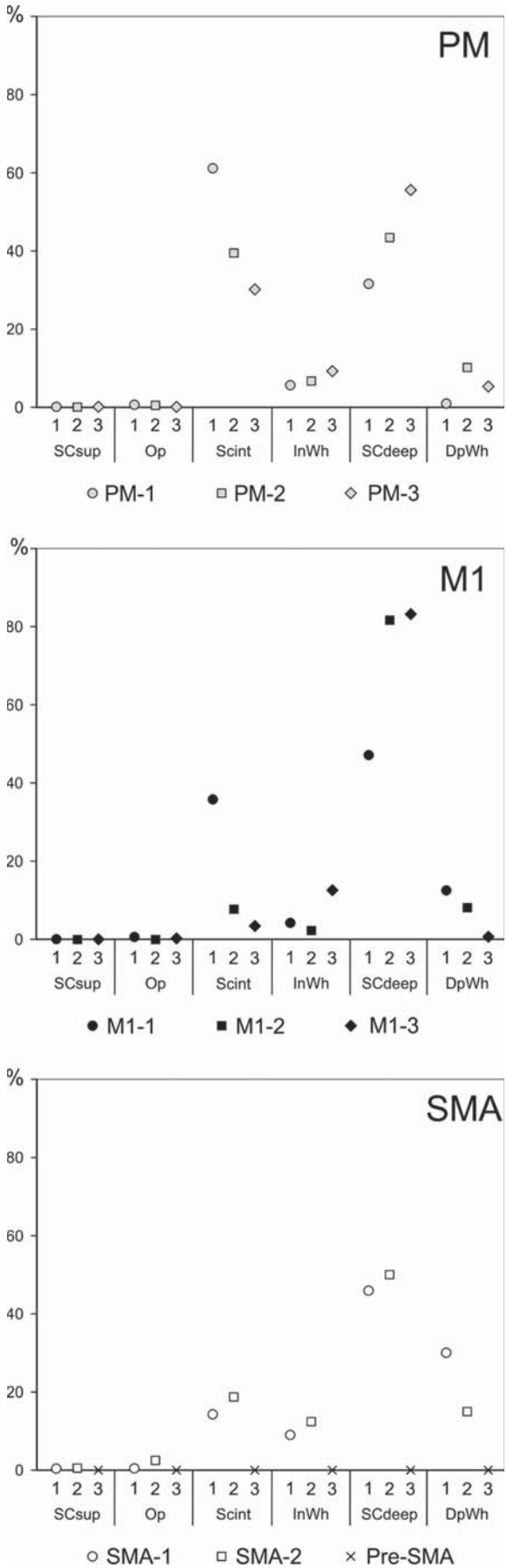

FIG. 6. For each motor cortical area injected with BDA, the scatter plots show the percentage distribution of the BDA-labelled axonal boutons across the six sub-regions of the superior colliculus (listed along the abscissa). In each monkey, the sum of all values is 100%. The distribution is based on the corrected numbers of boutons (Table 1). The bottom graph includes the data for SMA-proper (SMA-1 and SMA-2) and for Pre-SMA. See list of abbreviations.

circuits in the deeper layers of the SC. One may speculate that the motor corticotectal projection provides the SC with an efferent copy of the voluntary movement programs. This efferent copy could be used locally for sensorimotor integration in the SC rather than as an indirect route from the cerebral cortex to spinal motoneurons via the tectum. For M1, such motor influence on the SC appears to be focused on the orofacial representation (Tokuno *et al.*, 1995), whereas it may involve more extensive body part representations from the PM and SMA (Borra *et al.*, 2010, 2014; Distler & Hoffmann, 2015; present study).

Acknowledgements

The authors thank Mrs Christine Roulin, Christiane Marti, Véronique Moret for their technical precious contributions to process the histological tissue and the animal caretakers (L. Bossy, J. Maillard, B. Bapst, B. Morandi and J. Corpataux). We thank Dr. Adjia Hamadjida, Dr. J. Tanné and Dr. D. Boussaoud for their contribution to some of the BDA injections. Thanks are due to Dr. Michael Harvey and Mrs Alexandra Hickey for proofreading the English in the final version of the manuscript. The present study was financially supported by Swiss National Science Foundation (SNF) grants to EMR, numbers 110005, 132465, 144990, 149643; grant Sinergia SNF number CRSII3_160696, and the Swiss Primate Competence Centre for Research (SPCCR, www.unifr.ch/spccr).

Conflict of interest

The authors declare to have no conflict of interest in relation to the present study.

Authors' contributions

EMR designed the study and performed the BDA injections. MF and EMR analysed the histological sections. MF and EMR drafted the manuscript.

Data accessibility

The histological material (brain sections) is publicly available at the Swiss Primate Competence Centre for Research (SPCCR) on request to the corresponding author. The detailed reconstruction (equivalent of Figs 2–4) of the corticotectal projection in each monkey will be available in the Ph.D. thesis manuscript of Michela Fregosi, accessible in the repository of Ph.D. theses completed at the Faculty of Sciences of University of Fribourg (http://opac.rero.ch/gateway?).

Abbreviations

BDA, biotinylated dextran amine; CS, corticospinal; DpWh, deep white layer of SC; InWh, intermediate white layer of SC; M1, primary motor cortex; MGB, medial geniculate body; OP, optic nerve layer of SC; PAG, periacqueductal grey; PM, premotor cortex; PMRF, Ponto-Medullary Reticular Formation; PMv, ventral premotor cortex; PMd, dorsal premotor cortex; Pn, pontine nuclei; Pul, pulvinar nucleus of the thalamus; SC, superior colliculus; SCsup, superior layer of SC; SCint, intermediate layer of SC; SCdeep, deep layer of SC; SMA, supplementary motor area; SMA-proper, caudal part of SMA; pre-SMA, rostral part of SMA.

References

Abrahams, V.C. & Rose, P.K. (1975) Projections of extraocular, neck muscle, and retinal afferents to superior colliculus in the cat: their connections to cells of origin of tectospinal tract. *J. Neurophysiol.*, **38**, 10–18.

Barbas, H. & Garcia-Cabezas, M.A. (2015) Motor cortex layer 4: less is more. *Trends Neurosci.*, **38**, 259–261.

Borra, E., Belmalih, A., Gerbella, M., Rozzi, S. & Luppino, G. (2010) Projections of the hand field of the macaque ventral premotor area F5 to the brainstem and spinal cord. *J. Comp. Neurol.*, **518**, 2570–2591.

Borra, E., Gerbella, M., Rozzi, S., Tonelli, S. & Luppino, G. (2014) Projections to the superior colliculus from inferior parietal, ventral premotor, and ventrolateral prefrontal areas involved in controlling goal-directed hand actions in the macaque. *Cereb. Cortex*, **24**, 1054–1065.

Buford, J.A. & Davidson, A.G. (2004) Movement-related and preparatory activity in the reticulospinal system of the monkey. *Exp. Brain Res.*, **159**, 284–300.

Castiglioni, A.J., Gallaway, M.C. & Coulter, J.D. (1978) Spinal projections from the midbrain in monkey. *J. Comp. Neurol.*, **178**, 329–346.

Collins, C.E., Lyon, D.C. & Kaas, J.H. (2005) Distribution across cortical areas of neurons projecting to the superior colliculus in new world monkeys. *Anat. Rec. Part A*, **285**, 619–627.

Courtine, G., Bunge, M.B., Fawcett, J.W., Grossman, R.G., Kaas, J.H., Lemon, R., Maier, I., Martin, J. *et al.* (2007) Can experiments in nonhuman primates expedite the translation of treatments for spinal cord injury in humans? *Nat. Med.*, **13**, 561–566.

Davidson, A.G. & Buford, J.A. (2004) Motor outputs from the primate reticular formation to shoulder muscles as revealed by stimulus-triggered averaging. *J. Neurophysiol.*, **92**, 83–95.

Davidson, A.G. & Buford, J.A. (2006) Bilateral actions of the reticulospinal tract on arm and shoulder muscles in the monkey: stimulus triggered averaging. *Exp. Brain Res.*, **173**, 25–39.

Davidson, A.G., Schieber, M.H. & Buford, J.A. (2007) Bilateral spike-triggered average effects in arm and shoulder muscles from the monkey pontomedullary reticular formation. *J. Neurosci.*, **27**, 8053–8058.

Distel, H. & Fries, W. (1982) Contralateral cortical projections to the superior colliculus in the macaque monkey. *Exp. Brain Res.*, **48**, 157–162.

Distler, C. & Hoffmann, K.P. (2015) Direct projections from the dorsal premotor cortex to the superior colliculus in the macaque (Macaca mulatta). *J. Comp. Neurol.*, **523**, 2390–2408.

Dum, R.P. & Strick, P.L. (1991) The origin of corticospinal projections from the premotor areas in the frontal lobe. *J. Neurosci.*, **11**, 667–689.

Dum, R.P. & Strick, P.L. (1996) Spinal cord terminations of the medial wall motor areas in macaque monkeys. *J. Neurosci.*, **16**, 6513–6525.

Fregosi, M., Contestabile, A., Hamadjida, A. & Rouiller, E.M. (2017) Corticobulbar projections from distinct motor cortical areas to the reticular formation in macaque monkeys. *Eur. J. Neurosci.*, **45**, 1379–1395.

Freund, P., Wannier, T., Schmidlin, E., Bloch, J., Mir, A., Schwab, M.E. & Rouiller, E.M. (2007) Anti-Nogo-A antibody treatment enhances sprouting of corticospinal axons rostral to a unilateral cervical spinal cord lesion in adult macaque monkey. *J. Comp. Neurol.*, **502**, 644–659.

Fries, W. (1984) Cortical projections to the superior colliculus in the macaque monkey: a retrograde study using horseradish peroxidase. *J. Comp. Neurol.*, **230**, 55–76.

Fries, W. (1985) Inputs from motor and premotor cortex to the superior colliculus of the macaque monkey. *Behav. Brain Res.*, **18**, 95–105.

Gandhi, N.J. & Katnani, H.A. (2011) Motor functions of the superior colliculus. *Annu. Rev. Neurosci.*, **34**, 205–231.

He, S.-Q., Dum, R.P. & Strick, P.L. (1993) Topographic organization of corticospinal projections from the frontal lobe: motor areas on the lateral surface of the hemisphere. *J. Neurosci.*, **13**, 952–980.

He, S.-Q., Dum, R.P. & Strick, P.L. (1995) Topographic organization of corticospinal projections from the frontal lobe: motor areas on the medial surface of the hemisphere. *J. Neurosci.*, **15**, 3284–3306.

Innocenti, G.M., Dyrby, T.B., Andersen, K.W., Rouiller, E.M. & Caminiti, R. (2017) The Crossed Projection to the Striatum in Two Species of Monkey and in Humans: behavioral and Evolutionary Significance. *Cereb. Cortex*, **27**, 3217–3230.

Kneisley, L.W., Biber, M.P. & Lavail, J.H. (1978) A study of the origin of brain stem projections to monkey spinal cord using the retrograde transport method. *Exp. Neurol.*, **60**, 116–139.

Kuypers, H.G.J.M. (1981) Anatomy of descending pathways. In Brooks, V.B. (Ed.), *Handbook of Physiology (The Nervous System), Vol. II, Part 1*. Am. Physiol. Soc, Bethesda, MD, pp. 597–666.

Kuypers, H.G.J.M. & Lawrence, D.G. (1967) Cortical projections to the red nucleus and the brain stem in the rhesus monkey. *Brain Res.*, **4**, 151–188.

Lawrence, D.G. & Hopkins, D.A. (1976) The development of motor control in the Rhesus monkey: evidence concerning the role of corticomotoneuronal connections. *Brain*, **99**, 235–254.

Lawrence, D.G., Porter, R. & Redman, S.J. (1985) Corticomotoneuronal synapses in the monkey:light microscopic localization upon motoneurons of intrinsic muscles of the hand. *J. Comp. Neurol.*, **232**, 499–510.

Lemon, R.N. (2008) Descending pathways in motor control. *Annu. Rev. Neurosci.*, **31**, 195–218.

Lemon, R.N. (2016) Cortical projections to the red nucleus and the brain stem in the rhesus monkey. *Brain Res.*, **1645**, 28–30.

Lemon, R.N. & Griffiths, J. (2005) Comparing the function of the corticospinal system in different species: organizational differences for motor specialization? *Muscle Nerve*, **32**, 261–279.

Liu, J., Morel, A., Wannier, T. & Rouiller, E.M. (2002) Origins of callosal projections to the supplementary motor area (SMA): a direct comparison between pre-SMA and SMA-proper in macaque monkeys. *J. Comp. Neurol.*, **443**, 71–85.

Lock, T.M., Baizer, J.S. & Bender, D.B. (2003) Distribution of corticotectal cells in macaque. *Exp. Brain Res.*, **151**, 455–470.

Luppino, G., Matelli, M., Camarda, R. & Rizzolatti, G. (1993) Corticocortical connections of area F3 (SMA-proper) and area F6 (pre-SMA) in the macaque monkey. *J. Comp. Neurol.*, **338**, 114–140.

Markov, N.T., Ercsey-Ravasz, M.M., Ribeiro Gomes, A.R., Lamy, C., Magrou, L., Vezoli, J., Misery, P., Falchier, A. *et al.* (2014) A weighted and directed interareal connectivity matrix for macaque cerebral cortex. *Cereb. Cortex*, **24**, 17–36.

Monakow, K.H., Akert, K. & Kunzle, H. (1979) Projections of precentral and premotor cortex to the red nucleus and other midbrain areas in Macaca fascicularis. *Exp. Brain Res.*, **34**, 91–105.

Morecraft, R.J., Stilwell-Morecraft, K.S., Cipolloni, P.B., Ge, J., McNeal, D.W. & Pandya, D.N. (2012) Cytoarchitecture and cortical connections of the anterior cingulate and adjacent somatomotor fields in the rhesus monkey. *Brain Res. Bull.*, **87**, 457–497.

Morecraft, R.J., Stilwell-Morecraft, K.S., Ge, J., Cipolloni, P.B. & Pandya, D.N. (2015) Cytoarchitecture and cortical connections of the anterior insula and adjacent frontal motor fields in the rhesus monkey. *Brain Res. Bull.*, **119**, 52–72.

Nagy, A., Kruse, W., Rottmann, S., Dannenberg, S. & Hoffmann, K.P. (2006) Somatosensory-motor neuronal activity in the superior colliculus of the primate. *Neuron*, **52**, 525–534.

Nudo, R.J. & Masterton, R.B. (1988) Descending pathways to the spinal cord: a comparative study of 22 mammals. *J. Comp. Neurol.*, **277**, 53–79.

Nudo, R.J. & Masterton, R.B. (1989) Descending pathways to the spinal cord: II. Quantitative study of the tectospinal tract in 23 mammals. *J. Comp. Neurol.*, **286**, 96–119.

Nudo, R.J., Sutherland, D.P. & Masterton, R.B. (1993) Inter- and intra-laminar distribution of tectospinal neurons in 23 mammals. *Brain Behav. Evolut.*, **42**, 1–23.

Paxinos, G., Huang, X.F. & Toga, A.W. (2000). *The Rhesus Monkey Brain in Stereotaxic Coordinates*. Academic Press, London; San Diego.

Philipp, R. & Hoffmann, K.P. (2014) Arm movements induced by electrical microstimulation in the superior colliculus of the macaque monkey. *J. Neurosci.*, **34**, 3350–3363.

Riddle, C.N. & Baker, S.N. (2010) Convergence of pyramidal and medial brain stem descending pathways onto macaque cervical spinal interneurons. *J. Neurophysiol.*, **103**, 2821–2832.

Riddle, C.N., Edgley, S.A. & Baker, S.N. (2009) Direct and indirect connections with upper limb motoneurons from the primate reticulospinal tract. *J. Neurosci.*, **29**, 4993–4999.

Rouiller, E.M., Babalian, A., Kazennikov, O., Moret, V., Yu, X.-H. & Wiesendanger, M. (1994) Transcallosal connections of the distal forelimb representations of the primary and supplementary motor cortical areas in macaque monkeys. *Exp. Brain Res.*, **102**, 227–243.

Rouiller, E.M., Moret, V., Tanné, J. & Boussaoud, D. (1996) Evidence for direct connections between the hand region of the supplementary motor area and cervical motoneurons in the macaque monkey. *Eur. J. Neurosci.*, **8**, 1055–1059.

Rouiller, E.M., Tanné, J., Moret, V., Kermadi, I., Boussaoud, D. & Welker, E. (1998) Dual morphology and topography of the corticothalamic terminals originating from the primary, supplementary motor, and dorsal premotor cortical areas in macaque monkeys. *J. Comp. Neurol.*, **396**, 169–185.

Rouiller, E.M., Tanne, J., Moret, V. & Boussaoud, D. (1999) Origin of thalamic inputs to the primary, premotor, and supplementary motor cortical

areas and to area 46 in macaque monkeys: a multiple retrograde tracing study. *J. Comp. Neurol.*, **409**, 131–152.
Sakai, S.T., Davidson, A.G. & Buford, J.A. (2009) Reticulospinal neurons in the pontomedullary reticular formation of the monkey (Macaca fascicularis). *Neuroscience*, **163**, 1158–1170.
Schmidlin, E., Jouffrais, C., Freund, P., Wannier-Morino, P., Beaud, M.L., Rouiller, E.M. & Wannier, T. (2009) A case of polymicrogyria in macaque monkey: impact on anatomy and function of the motor system. *BMC Neurosci.*, **10**, 155.
Shook, B.L., Schlag-Rey, M. & Schlag, J. (1990) Primate supplementary eye field: I. Comparative aspects of mesencephalic and pontine connections. *J. Comp. Neurol.*, **301**, 618–642.
Soteropoulos, D.S., Williams, E.R. & Baker, S.N. (2012) Cells in the monkey ponto-medullary reticular formation modulate their activity with slow finger movements. *J. Physiol.*, **590**, 4011–4027.
Squire, L.R., Berg, D., Bloom, F.E., du Lac, S., Ghosh, A. & Spitzer, N.C. (2013). *Fundamental Neuroscience*, 4th Edn. Academic Press, Elsevier Science, Amsterdam, pp. 707.
Stein, B.E., Stanford, T.R., Ramachandran, R., Perrault, T.J. Jr & Rowland, B.A. (2009) Challenges in quantifying multisensory integration: alternative criteria, models, and inverse effectiveness. *Exp. Brain Res.*, **198**, 113–126.
Stuphorn, V., Hoffmann, K.P. & Miller, L.E. (1999) Correlation of primate superior colliculus and reticular formation discharge with proximal limb muscle activity. *J. Neurophysiol.*, **81**, 1978–1982.
Stuphorn, V., Bauswein, E. & Hoffmann, K.P. (2000) Neurons in the primate superior colliculus coding for arm movements in gaze-related coordinates. *J. Neurophysiol.*, **83**, 1283–1299.
Tanné-Gariépy, J., Boussaoud, D. & Rouiller, E.M. (2002a) Projections of the claustrum to the primary motor, premotor, and prefrontal cortices in the macaque monkey. *J. Comp. Neurol.*, **454**, 140–157.
Tanné-Gariépy, J., Rouiller, E.M. & Boussaoud, D. (2002b) Parietal inputs to dorsal versus ventral premotor areas in the macaque monkey: evidence for largely segregated visuomotor pathways. *Exp. Brain Res.*, **145**, 91–103.
Tokuno, H., Takada, M., Nambu, A. & Inase, M. (1995) Direct projections from the orofacial region of the primary motor cortex to the superior colliculus in the macaque monkey. *Brain Res.*, **703**, 217–222.
Werner, W. (1993) Neurons in the primate superior colliculus are active before and during arm movements to visual targets. *Eur. J. Neurosci.*, **5**, 335–340.
Werner, W., Hoffmann, K.P. & Dannenberg, S. (1997a) Anatomical distribution of arm-movement-related neurons in the primate superior colliculus and underlying reticular formation in comparison with visual and saccadic cells. *Exp. Brain Res.*, **115**, 206–216.
Werner, W., Dannenberg, S. & Hoffmann, K.P. (1997b) Arm-movement-related neurons in the primate superior colliculus and underlying reticular formation: comparison of neuronal activity with EMGs of muscles of the shoulder, arm and trunk during reaching. *Exp. Brain Res.*, **115**, 191–205.
Wurtz, R.H. (2009). Superior colliculus. In Squire, L.R. (Ed.), *Encyclopedia of Neuroscience*. Academic Press, Oxford, pp. 627–634.